GEOPHYSICS, VOL. 53, NO. 4 (APRIL 1988); P. 537–545, 9 FIGS., 4 TABLES.

Time-domain electromagnetic detection of a hidden target

David C. Bartel* and A. Becker*

ABSTRACT

Numerical modeling of the time-domain electromagnetic (EM) step response of a vertical tabular target hidden beneath a thin conductive overburden reveals that the target's presence may be detected only during a well-defined time window. In a situation where the secondary magnetic field is sensed by an airborne system equipped with horizontal coaxial dipoles, a conductance contrast of about ten between the target and the overburden is needed to ensure target detection. This value will, of course, vary with the size and depth of the target and, to a lesser extent, with the geometry of the system. In general, the time at which the window opens is a function of the geometrical parameters of the target, the height of the system, and the conductance of the overburden. For a given target, its width (defined as the ratio of the time of closure to the time of opening) is only a function of the conductance contrast between the target and the overburden. While the target signal is visible, one observes a maximum value of the target-to-overburden response ratio. The time at which this occurs is mainly controlled by the conductance of the target.

The presence of the overburden causes the target signal to build up gradually before decaying toward zero. However, once the target signal dominates the overburden response, the signal can be approximated by a simple exponential decay over the time range of interest. The time constant of this decay is determined by the size and conductance of the target. Using this model, it is easy to relate the magnetic field step response calculated here to the response observable with a conventional EM system that transmits a primary field pulse of finite duration and detects the time derivative of the secondary magnetic field.

INTRODUCTION

Time-domain electromagnetic (TEM) measurements constitute a widely used technique for the discovery of buried conductive bodies, particularly those hidden by conductive overburden. The process of target detection is complicated because electromagnetic (EM) induction in the target is influenced by the presence of the overlying material. Target detection must be mastered, however, because it is central to assessing the usefulness of a given TEM system in the search for a particular conductive target. As observed by Buselli (1980) and Spies (1980a, b) in their studies of the Australian Elura deposit, the target signal is observable only during a given time interval, or "window," set with respect to the instant of primary field extinction. At early and late times outside of this interval, the overburden response dominates the observed signal. In fact, the presence of the overburden reduces the rate of primary flux change at the target so that the early-time target signal is severely attenuated. At late times, the overburden response, which falls off as an inverse power of time, once again dominates the target signal.

The definition of the time window through which the target signal may be observed is the key to successful exploration in areas of conductive overburden. Once the window is specified, one can predict whether a given TEM system will detect a proposed target. Kaufman (1981) addressed this problem by considering the response of a buried spheroid to a coaxial coincident-loop system. Assuming that the responses of the target and the overburden are essentially decoupled at the time when the target response is detected, he was able to demonstrate theoretically the presence of the experimentally observed time window and to predict the observation time when the target-to-overburden response ratio (TOR) is at a maximum. In a more extensive study, Eaton and Hohmann (1987) used a numerical model to examine the TOR of a prismatic target in a conducting host rock and covered by a conductive overburden block. Eaton and Hohmann computed TORs for various transmitter-receiver configurations; their re-

Presented in part at the 56th Annual International Meeting, Society of Exploration Geophysicists, 1986. Manuscript received by the Editor June 5, 1986; revised manuscript received September 11, 1987.
*Engineering Geoscience, 414 Hearst Mining Building, University of California, Berkeley, CA 94720.

sults agreed with those of Kaufman (1981) and of McCracken et al. (1986).

We propose to examine the detection problem for a typical Precambrian Shield mineral deposit located under moderate conductive cover. The average size of such a mineral deposit was determined by Bosschart and Seigel (1965) to be approximately 300 by 300 m. As an example of this situation, consider the scale-model response of a vertical 300 by 300 m tabular body whose conductance is 30 S and which is located 50 m beneath a square, thin conductive sheet that is 2.2 km wide, with a conductance of 3 S. For experimental reasons, the transmitter and receiver coils are mounted in a horizontal coaxial dipole configuration 50 m above the overburden sheet and separated by 100 m. Except for the coil configuration, which does not have an industrial counterpart, the rest of the scale-model apparatus is similar to the INPUT® airborne TEM system as described by Lazenby (1973). The transmitter waveform is a half-sine wave of alternating polarity with a pulse duration of 1.8 ms and a waveform period of 9.5 ms. The secondary field response is sampled during six time gates or channels after turnoff of the transmitter current. These channels are centered at 0.26, 0.43, 0.7, 1.05, 1.5, and 2.0 ms. The scale-model anomaly is shown in Figure 1 with each channel displayed in parts per million (ppm) of the primary field at various sensitivities as required for display. The system geometry is shown in Figure 2, where it should be noted that the areal extent of the scale-model overburden is limited.

The target signature is clearly observed in the later channels and appears in the center of Figure 1 directly above the target located at the 0 km mark. The target is flanked by anomalies related to the edges of the overburden. Because the scale-model apparatus measures the voltage induced in the receiver by the changing secondary field, the target anomaly in channel 1 is negative, since it corresponds to a growing secondary magnetic field. Even though the target signal observed in channel 6 is smaller than that seen in channel 5, the TOR in the later channel is nearly twice as big.

The problem of predicting and/or evaluating the response of the TEM system can thus be reduced to establishing a means for deciding the time at which the target signal constitutes a significant fraction of the overburden signal, and, more importantly, the time at which the TOR is a maximum. In our scale-model illustration, channel 3 probably satisfies the first criterion; unfortunately, the limited time window of the detector does not allow for observation of the target signal at the maximum TOR. Because the overburden in Figure 1 is uniform, the anomaly in channel 3 is clearly marked even though the TOR is small. In practice, the overburden is usually not uniform, and a TOR of at least unity is necessary for detection of the target in the presence of geologic noise.

A solution to this problem of determining the maximum TOR can be found by a combination of analytical and numerical techniques. The magnetic field step response for an overburden of infinite extent is known (Grant and West, 1965, p. 498); while the target response can be obtained numerically with the help of a computer program originated by P. Weidelt (1981).

® Trademark of Barringer Research Ltd.

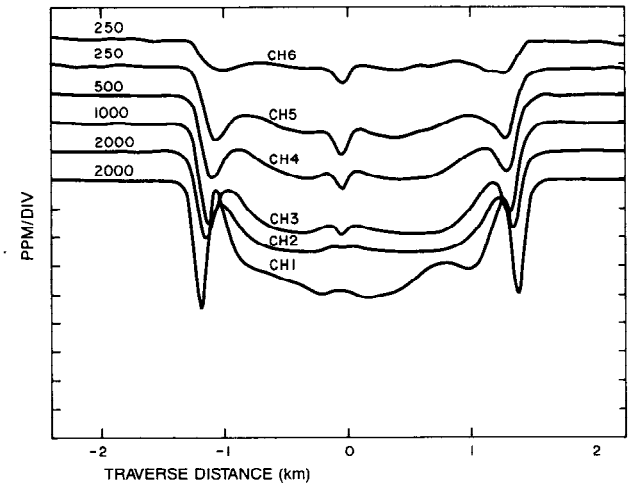

FIG. 1. Scale-model example for the INPUT system equipped with vertical coaxial transmitter and receiver coils; transmitter-receiver altitude = 50 m, target depth = 50 m, overburden conductance = 3 S, target conductance = 30 S, target size is 300 by 300 m. ppm refers to parts per million of the primary field; numbers above each profile refer to the ppm per division for that profile; a positive response is downward. Vertical target located at 0 km.

COMPUTATIONAL TECHNIQUES

Model geometry

As shown in Figure 2, the model considered here is a 300 by 300 m vertical, tabular target of variable conductance $\sigma_2 s_2$, situated in a host rock of negligible (0.1 mS/m) conductivity. The host rock is covered by a thin sheet of conductive overburden of conductance $\sigma_1 s_1$, which is varied so that the effects of changes in the conductance ratio may be studied. The distance D between the top of the target and the ground surface can also be varied, but because of restrictions in the numerical calculations, the target and overburden cannot be in electrical contact. For this study, we have elected to use a maximum coupled coaxial system with horizontal coil axes aligned parallel to the line of flight. A constant flight height of 50 m is

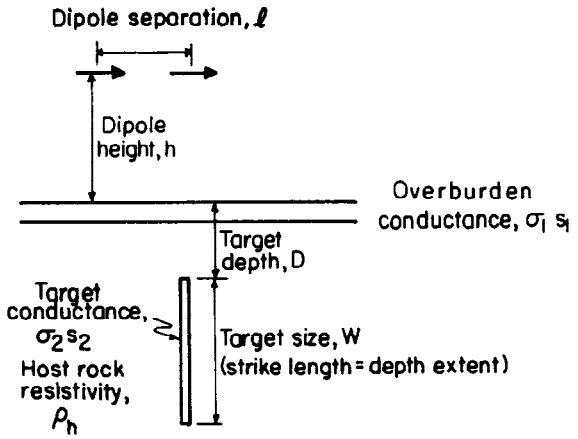

FIG. 2. Model geometry cross-section.

used for all models, but the height-to-coil separation (h/ℓ) ratio may vary. Considerable simplification is brought to the problem by giving special attention to the case where the h/ℓ ratio is very large. In all cases, the anomaly is observed with the center of the system located directly above the centerline of the target.

Thin-sheet overburden

The analytical solution for the time-domain magnetic field response of a dipole above an infinite, thin sheet in free space is given by Grant and West (1965, p. 498). Here only the conductance of the sheet has any meaning, rather than the separate conductivity and thickness. The secondary magnetic field due to instantaneous current extinction in a transmitting dipole located at coordinates (0, 0, h) with a receiving dipole at (x, y, z) above a thin sheet of conductance $\sigma_1 s_1$ is given by Grant and West (1965, p. 500) as

$$\mathbf{H}^s(t) = \frac{-1}{4\pi}\left(\nabla\left\{\mathbf{m}\cdot\nabla_0\left[(x-x_0)^2+(y-y_0)^2 + \left(z+z_0+\frac{2t}{\mu_0\sigma_1 s_1}\right)^2\right]^{-1/2}\right\}\right). \quad (1)$$

If equation (1) is calculated for the specific case of horizontal coaxial dipoles, it becomes

$$H_x^s(t) = \frac{-m(r_t^2 - 3\ell^2)}{4\pi r_t^5}, \quad (2)$$

where

$$r_t^2 = \ell^2 + 4\left(h + \frac{t}{\mu_0\sigma_1 s_1}\right)^2. \quad (3)$$

The height of the transmitting and receiving dipoles above the thin sheet is h and their separation is ℓ. The dipole strength of the transmitter is m; μ_0 is the magnetic permeability of free space; and $\sigma_1 s_1$ is the conductance of the thin sheet.

Finally we note that for a closely coupled system ($\ell \ll h$), equation (2) can be approximated by

$$H_x^s(t) \approx \frac{-m}{4\pi(2h)^3(1+\tau_1)^3}, \quad (4)$$

where

$$\tau_1 = \frac{t}{\mu_0\sigma_1 s_1 h}. \quad (5)$$

For late times or large values of τ_1, the overburden falls off as t^{-3}.

The above relationships are only correct when the overburden sheet is sufficiently thin for any induced currents to flow only in the plane of the sheet and to be uniformly distributed across its thickness. These conditions certainly hold for normalized times greater than unity (Kaufman, 1981) and the overburden response can be simplified again to read

$$H_x^s(t) \approx \frac{-m}{4\pi(2h)^3\tau_1^3} \approx \frac{-m}{32\pi}\left(\frac{\mu_0\sigma_1 s_1}{t}\right)^3, \quad (6)$$

eliminating dependence on the altitude of the system.

Target signal

The computer program used to calculate the target signal was originally developed by Weidelt (1981). It allows for numerical computation of the response of a thin tabular body of a given conductance in a conducting host rock. The host rock may in turn be covered by a conducting overburden of some specified thickness. Although no direct electrical contact is made between the overburden and the target, full EM coupling is maintained between the target and all enveloping formations. A dipole source located above the overburden is used to generate a primary magnetic field at a chosen frequency, while the secondary field is sensed by a similarly positioned detector.

Labeled "SHEET" by its originator, this program calculates both the complete model response and the response of the layered geologic model (host rock + overburden) in the absence of the target. Subtraction of these two quantities for a number of different frequencies results in the definition of the frequency-domain target response. The process of obtaining the desired time-domain magnetic field step response of the target is now completed with a fast Fourier transform (FFT) subroutine. The accuracy of the transformed numerical data was found to be satisfactory through comparisons with scale-model results and other numerical programs.

NUMERICAL RESULTS

Conductance contrast

To gain an understanding of the induction process, we first examine the target signal as a function of the conductance contrast between the target and the overburden. This is done in Figure 3, where the normalized secondary field is plotted as

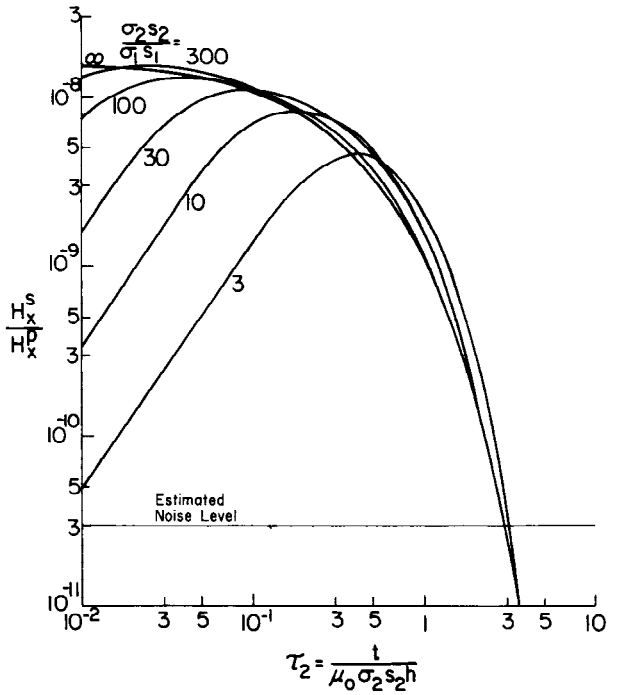

FIG. 3. Target response as a function of the normalized time of the target for different conductance contrasts; $h/\ell = 50$, $h = 50$ m, $D = 30$ m, $W = 300$ m, with the system centered over the target.

a function of normalized time. Following Spies (1976, 1980a), the time axis is normalized with respect to the target conductance, while the amplitude of the secondary field is normalized by the primary field measured at the receiver position. For purposes of comparison, we include the free-space response for the same target calculated using the PLATE program (Dyck et al., 1980). This response appears as the curve identified with an infinite target-to-overburden conductance contrast. All calculations were done for a system height of 50 m, an h/ℓ ratio of 50, and a target depth of 30 m.

Initially, the buried target signal differs significantly from its free-space counterpart. Unlike the latter, the buried signal does not rise instantaneously to counteract the extinction of the primary field. Instead, it rises at a given rate, reaches a maximum, and only then becomes asymptotic to its free-space value. Its initial rate of increase can be shown to be proportional to t^2, falling to the $t^{3/2}$ rate shown at the start of the time range of observation. The time of the maximum target signal is dependent upon the target-to-overburden conductance contrast. At times the buried target response slightly exceeds its free-space value, probably because of minor galvanic enhancement provided by the nonzero conductivity of its host rock. Finally, we note that the observable late-stage (large τ_2) decay of the target response is almost exponential. It is independent of overburden conductance and nearly coincides with the free-space value of the target signal.

To put these results in perspective with regard to target detection, it is helpful to replot the results on a time scale normalized by the overburden conductance. Figure 4 includes this plot and the overburden response, indicated by the dashed line labeled "thin sheet," and for purposes of comparison, an exponential function exp $(-\tau_1/60)$. The target signal exceeds the overburden response in an identifiable time window when the target-to-overburden conductance contrast is at least 10. We label the time point where the target response first exceeds the overburden response as τ_{early}, the time of maximum target-to-overburden response ratio (TOR) as τ_0, and the point where the overburden response again prevails as τ_{late}. It is of immediate interest to note the relative independence of τ_{early} from the target conductance.

The signal window sought here can be rendered more evident by considering the TOR as a function of time and conductance contrast as shown in Figure 5. It is the conductance contrast that has the main influence on the maximum observable TOR. Conversely, the TOR at low τ_1 values is largely independent of this quantity. If the TOR curves were to be plotted versus τ_2, rather than against τ_1, we would see that τ_0 (the time of maximum TOR) is directly proportional to the conductance of the target.

The intimate relationship between τ_0 and the target conductance results in the observation that the target signal will fall to about 3 percent of its free-space induction limit value by the time τ_0 is reached. McCracken et al. (1986) also eached this conclusion in defining the time of maximum TOR when the overburden response decays as t^3. Thus, the time window during which the target signal may be observed is effectively bounded by τ_{early} and τ_0 even though the target signal dominates the overburden response out to τ_{late}. In further support of this remark, we note that the relative signal level at time τ_0 is about 5×10^{-10} for a 50 m deep conductor. While this level is well above a relative estimated noise level of 3×10^{-11} for this type of system, the signal is unlikely to be observable later than τ_0.

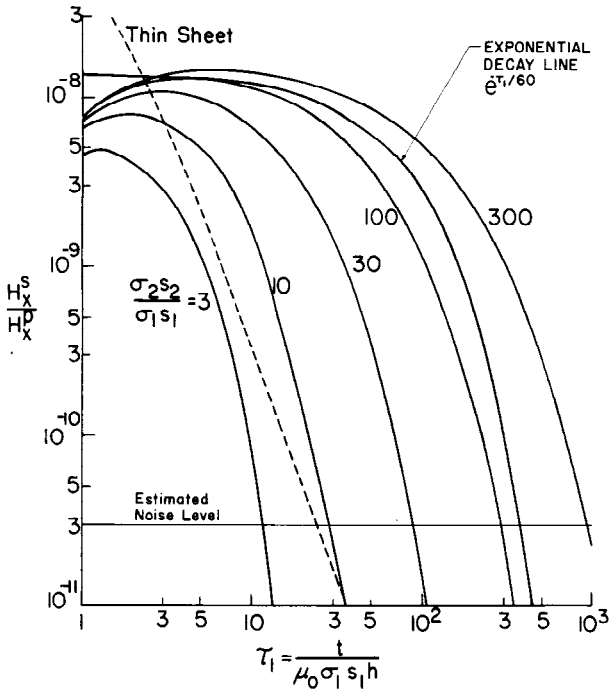

FIG. 4. Target response as a function of the normalized time of the overburden [equation (5)] for $h/\ell = 50$ and $D = 30$ m, $h = 50$ m, $W = 300$ m, with the system centered over the target.

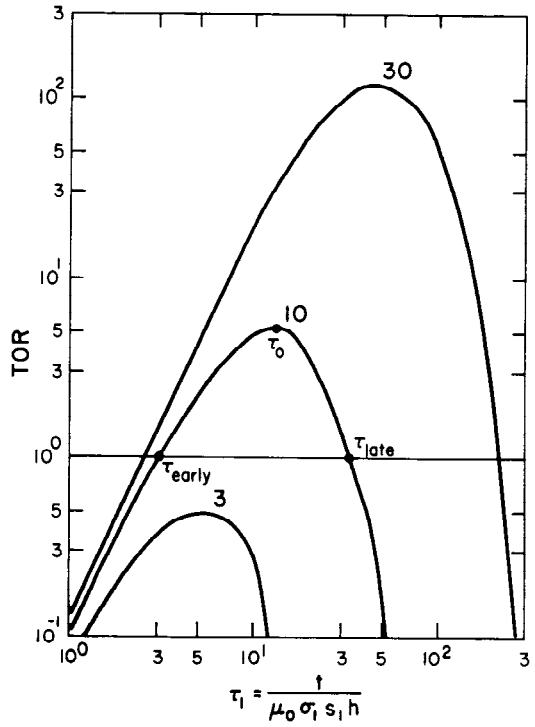

FIG. 5. TOR as a function of the normalized time of the overburden for $h/\ell = 50$ and $D = 30$ m; curves are for various $\sigma_2 s_2/\sigma_1 s_1$ contrasts, $h = 50$ m, $W = 300$ m, with the system centered over the target.

Table 1. Target detection for $h/\ell = 50$, $D = 30$ m; $h = 50$ m, $W = 300$ m. τ_{early} and τ_{late} refer to the τ_1 values where the target-to-overburden response ratio (TOR) equals 1.0. τ_0 is the τ_1 value where the maximum TOR occurs. The profile position for these values is where the transmitting and receiving dipoles are centered over the target (see curves in Figure 4).

Target detectability: $h/\ell = 50$, $D = 30$ m

$\sigma_2 s_2/\sigma_1 s_1$ contrast	τ_{early}	τ_{late}	τ_0	TOR_{max}
3	—	—	5.2	0.5
10	3.0	36.	14.	5.4
30	2.5	200	46.	120
100	2.4	900	160	3 000
300	2.4	3400	460	72 000

For further reference, it is useful to extract the critical points from the data shown in Figure 4. Table 1 presents values of τ_{early}, τ_0, and τ_{late} as a function of the target-to-overburden conductance contrast. Values of the first two parameters are available directly from Figure 4, while extrapolation was used to obtain values of τ_{late} for large conductance contrasts.

Target depth

It is known that for a closely coupled coil configuration, free-space target signals show an approximate inverse cubic relationship between the anomaly amplitude and the target depth below the transmitter-receiver system (Gupta Sarma and Maru, 1971; Mallick, 1972b). The buried target response can also be expected to follow this power-law relationship at large τ_1 values, because in this region the target response is virtually identical to its free-space value. Figure 6 shows the peak target response amplitude and τ_{early} as a function of depth; as expected, an inverse cubic relationship is also observed for the peak amplitude of the buried target response. The relationship may not hold, however, at small τ_1 values because of the effects of the overburden. Obviously, as the target becomes shallower, τ_{early} decreases. It is controlled mostly by the depth of the target and is approximately related to $(h + D)^{3/2}$; τ_0, on the other hand, is largely independent of the target depth.

Geometry of the system

Because both the overburden and target responses change with the h/ℓ ratio, the ability to detect the target also varies with this parameter. Typical overburden response for a high h/ℓ ratio ($h/\ell = 50$) is shown as curve (a) in Figure 7. Of more interest is the low h/ℓ ratio regime, when $h/\ell < 1/\sqrt{2}$ and the overburden response is initially opposite in sign to its late-stage decay. The sign change occurs when $(h/\ell)(1 + \tau_1) = 1/\sqrt{2}$. Typical overburden response for this regime ($h/\ell = 0.5$) is shown in Figure 7 as curve (b). As may be expected, in both cases the late-stage decay of the overburden response is proportional to t^{-3}. Note that here the secondary field is normalized by $m/2\pi$, thereby largely eliminating the effect of the dipole separation ℓ. The peak overburden response [curves (a) and (b) in Figure 7] is greatly attenuated by a reduction in the

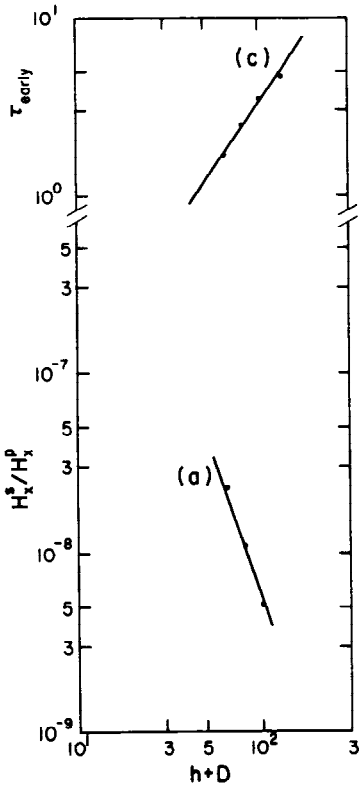

FIG. 6. Effect of the depth of the target on response amplitude and τ_{early} for $\sigma_2 s_2/\sigma_1 s_1$ contrast = 30, $h/\ell = 50$, $h = 50$ m, $W = 300$ m, with the system centered over the target. (a) maximum target signal, line corresponds to $(h + D)^{-3}$. (c) change in τ_{early} with depth, line corresponds to a variation with $(h + D)^{-3/2}$.

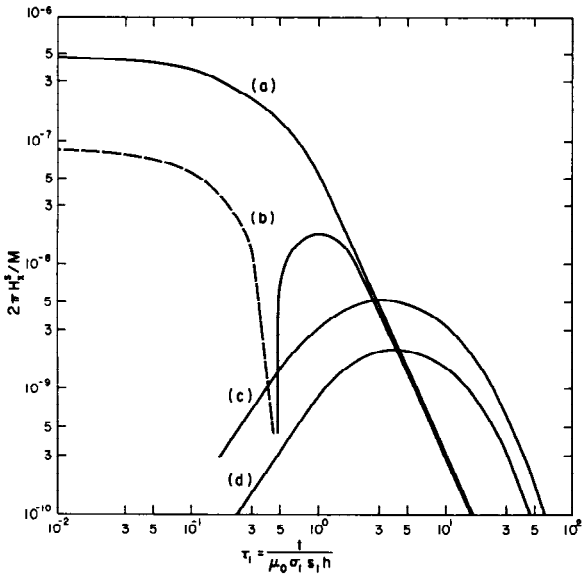

FIG. 7. Effect of system geometry for $h = 50$ m, $\sigma_2 s_2/\sigma_1 s_1$ contrast = 30, $D = 50$ m, $W = 300$ m, with the system centered over the target. (a) and (b) overburden response curves for $h/\ell = 50$ and 0.5, respectively; (c) and (d) target response curves for $h/\ell = 50$ and 0.5, respectively.

h/ℓ ratio. The target signal amplitudes [curves (c) and (d) in Figure 7], shown for a conductance contrast of 30, also decrease with the h/ℓ ratio, but this attenuation is related to the increased distance from the top of the target to the receiving dipole. At the point of the maximum anomaly, the receiving dipole is a distance $[(h + D)^2 + (\ell/2)^2]^{1/2}$ away from the top of the target and the anomaly amplitude is related to this distance cubed.

The detection statistics presented in Table 2 for a conductance contrast of 30 and a target depth of 50 m show variations in τ_{early} and the maximum TOR with different h/ℓ ratios. The value of τ_0 appears to be relatively invariant, but significant changes in τ_{early} occur when the h/ℓ ratio is less than one. The shape of the target anomaly profile for high h/ℓ ratios is a simple peak, whereas for low h/ℓ ratios the peak over the target has negative side lobes. The TOR in this case should thus be defined as the ratio of the peak-to-peak amplitude of the target response to the overburden response. For an h/ℓ ratio change from 50 to 0.5 (maintaining a constant h), the value of the maximum TOR decreases by approximately a factor of 2.

PRACTICAL CONSIDERATIONS

With the exception of the UTEM system (Lamontagne, 1975; West et al., 1984), conventional systems do not measure the electromagnetic step response of the Earth. Usually the transmitter current consists of a current pulse with finite length and a finite extinction time, and most EM systems measure the voltage induced in a receiver coil rather than measuring the observed magnetic field itself. The effects of a finite pulse length and late-time voltage measurements on target detection can be evaluated, however, with some elementary approximations. In particular, let us assume that in the time range of interest the target signal may be represented by a pure exponential decay of the form $Ae^{-\tau_1/\zeta}$, while the overburden response decreases with time according to an inverse power law governed by an exponent v. Our work, and that of Lamontagne (1975) and of Bartel and Hohmann (1985), show that a suitable empirical value for the target time constant is

$$\zeta = \frac{\sigma_2 s_2 W}{10\,\sigma_1 s_1 h}. \tag{7}$$

Table 2. Target detection for $\sigma_2 s_2/\sigma_1 s_1$ contrast = 30, D = 50 m, h = 50 m, W = 300 m, and the system is centered over the target (except as noted).

Target detectability: $\sigma_2 s_2/\sigma_1 s_1$ contrast = 30, D = 50 m			
h/ℓ ratio	τ_{early}	τ_0	TOR_{max}
50	3.5	52.	48.
25	3.5	48.	44.
5	3.4	46.	40.
1	3.8	48.	33.
0.5	4.9	48.	21. 22.*

*TOR_{max} defined from peak-to-peak amplitude; see text.

These assumptions appear to be validated by experimental results (McCracken et al., 1986), so that the expected values for τ_0 should be given by

$$\tau_0 = \nu\zeta. \tag{8}$$

For the magnetic field step response, the overburden exponent v is 3. Using the values of τ_0 in Tables 1 and 2, we find the resulting values of ζ to be in reasonable agreement with those calculated using equation (7), while the small systematic discrepancy between the values of ζ calculated with equation (7) and those using the data in Tables 1 and 2 can be ascribed to the empirical definition of the time constant ζ [equation (7)].

Pulse length

To study the effect of a finite pulse width, we examine the influence of a rectangular pulse width of normalized duration Δ. The pulse length is normalized as in equation (5), so that the transient field at some normalized time τ now contains contributions from the trailing and leading edges of the pulse. As before, we assume that the target signal has an exponential decay ($e^{-\tau/\zeta}$) and that the overburden response decays according to a power law ($\tau^{-\nu}$). Thus, the observed TOR when using a finite current pulse is as follows:

$$TOR_{modified} = \frac{1 - e^{-\Delta/\zeta}}{1 - \left(1 + \frac{\Delta}{\tau}\right)^{-\nu}}\, TOR_{original}. \tag{9}$$

For targets beneath conductive overburden, equation (9) can be expected to hold after the target response peaks.

The modifying factor on the original TOR as a function of Δ/ζ and Δ/τ using $\nu = 3$ is examined in Figure 8. There are three basic regions: first, a region corresponding to Δ/ζ and Δ/τ values that are both much greater than one. Here, the

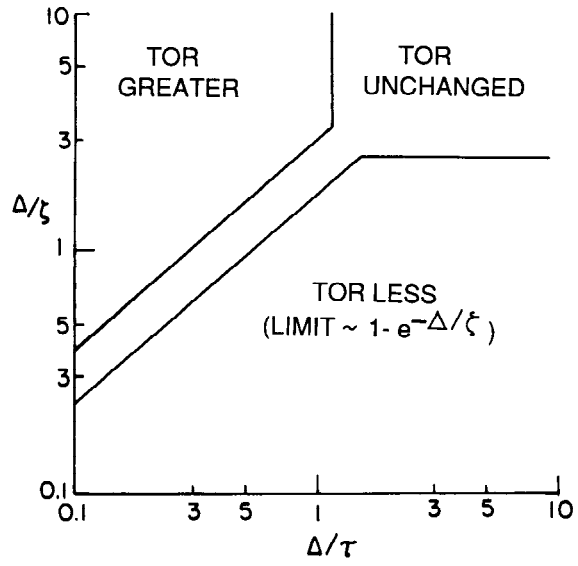

FIG. 8. Effect on TOR of current pulse length as a function of normalized measurement time and the time constant of the target [see equation (10)]. The overburden response is assumed to decay as t^{-3} [see equation (2)].

TOR is essentially unchanged. In the second region, where Δ/τ is large but Δ/ζ is small, the TOR is modified by a factor between $1 - e^{-\Delta/\zeta}$ and unity. In the third region when Δ/ζ is large and Δ/τ is small, the TOR can be enhanced. However, in a practical sense, this last situation is unlikely to occur often because the signal strength when $\Delta/\tau < 1$ is likely to be very low.

Voltage measurements

Most EM field systems measure the voltage induced in a receiver coil rather than the detected magnetic field. Because the observed voltage response is proportional to the time derivative of the magnetic field response, the response of a target beneath overburden will show a change in sign as the secondary field first grows, then decays. This phenomenon is shown in Figure 9, where the voltage responses of the target and overburden for a conductance contrast of 30 ($h/\ell = 50$ and $D = 30$ m) are compared. The late-stage (large τ_1) voltage response for a thin-sheet overburden is proportional to t^{-4}, as could be expected by taking the time derivative of equation (2). Target detection statistics for the voltage response as a function of the $\sigma_2 s_2/\sigma_1 s_1$ contrast are given in Table 3, where, as predicted by McCracken et al. (1986), τ_0 approximately equals four times the normalized time constant ζ.

If we again assume an exponential decay for the target response and a power-law decay for the overburden, then the late-time change in the TOR for a voltage detector is

$$\mathrm{TOR}_{\mathrm{modified}} = \left(\frac{\tau}{\sqrt{\zeta}}\right)\mathrm{TOR}_{\mathrm{original}}. \qquad (10)$$

Here it is evident that the voltage response can result in a higher TOR than the magnetic field response; thus the assertions of Gupta Sarma et al. (1976) and Mallick (1978) of a greater relative magnetic field target signal than voltage response for targets beneath overburden may not hold in all cases.

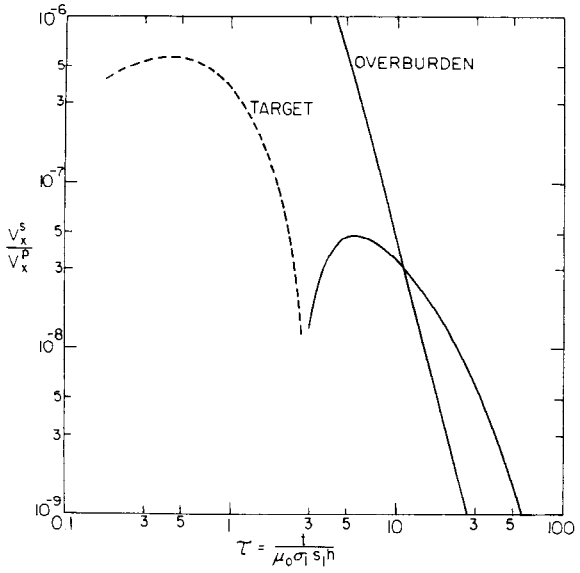

FIG. 9. Target and overburden voltage responses obtained using program SHEET; $h/\ell = 50$, $h = 50$ m, $\sigma_2 s_2/\sigma_1 s_1$ contrast = 30, $D = 30$ m, $W = 300$ m, with the system centered over the target.

Table 3. Voltage response target detection versus $\sigma_2 s_2/\sigma_1 s_1$ contrast for $h/\ell = 50$, $D = 30$ m; $h = 50$ m, $W = 300$ m, where the system is centered over the target.

Target detectability for voltage response: $h/\ell = 50$, $D = 30$ m			
$\sigma_2 s_2/\sigma_1 s_1$ contrast	τ_{early}	τ_0	$\mathrm{TOR}_{\mathrm{max}}$
10	—	18.	0.24
30	11.	68.	17.
100	8.4	190	1900

Scale-model demonstration

Now we have the tools for computing the TOR for an actual electromagnetic system such as that used to generate the scale model shown in Figure 1. As stated above, this equipment resembles the INPUT system as described by Lazenby (1973), with the exception of the 1.8 ms current pulse length and the vertical coaxial transmitter and receiver coils. The scale-model system senses the receiver voltage, so we must incorporate that modification [equation (10)], along with the effect of a finite current pulse [equation (9)] into our predictions of the TOR. There will also be minor effects related to the finite period of the waveform (9.5 ms for the scale-model system) and to the half-sine shape of the transmitter pulse, both of which are omitted. Previous work, however, suggests that the ratio between the time constant of the target and current pulse length should be in the range of 0.1 to 1.0 for the half-sine pulse response to resemble closely the magnitude of the step turnoff response (Mallick, 1972a; Becker et al., 1984).

To reiterate, the scale-model example shown in Figure 1 simulates a target underneath an overburden of large extent. The conductance contrast is approximately 10; the h/ℓ ratio is 0.5; and the target depth below the surface is 50 m. We aim to predict the TOR for channels 4 to 6 because at those observation times the target response is exponentially decaying and the finite extent of the overburden is not critical. The changes in the level of the overburden response evident on channel 1 are due to a slight uneveness in the overburden sheet surface but do not affect the late-time response. For this set of parameters, the maximum TOR for the magnetic field step response is determined with program SHEET to be 1.8. This value must be corrected for the finite current pulse length and voltage measurement using equations (9) and (10). An additional correction is needed because the INPUT measurements are not made at the time of the maximum TOR. Determination of that correction can be made from Figure 5. While the curves here are not for this model, they shift only vertically for changes in the system geometry or target depth, so that the relative value (with respect to $\mathrm{TOR}_{\mathrm{max}}$) of the TOR at a particular τ_1 can be determined.

The target time constant to be used in equations (9) and (10)

can be estimated from equation (7), which yields $\zeta = 6$ for the present model. This estimate of ζ may actually be a little high for this particular scale model, but it is a good starting point. The current pulse length for this example is also normalized by $\mu_0 \sigma_1 s_1 h$ to give $\Delta = 7.9$.

A summary of the necessary corrections and the calculated TORs is given in Table 4. The TOR for the scale model can be determined from Figure 1 using the peak-to-peak amplitude of the target response (since $h/\ell < 1$). The SHEET program was also run for the actual scale-model parameters (including the periodic half-sine waveform, but not the finite size of the overburden sheet), and the results also included in Table 4. The scale model values (TOR_{scale}) and SHEET program values (TOR_{SHEET}) for the response ratio agree within the errors of the two methods and coincidentally verify the accuracy of the basic SHEET data. The values for TOR_{pred} agree with the other two methods of calculation better at later times (i.e., channel 6) because the response decays of the target and overburden more closely resemble the assumed exponential decay and a power-law decay, respectively.

CONCLUSIONS

Having examined the problem of target detection in areas of conductive overburden, we find that our results agree well with the experimental observations and theoretical predictions made by others (Spies, 1980a, b; Kaufman, 1981). The outstanding feature of this problem is the clear definition of a temporal window through which the target may be observed. Unlike the case of a target located in a conducting host rock (Rai, 1985), where its signal may be observed undisturbed at intermediate to late times, with a conductive overburden the target signal can be observed after a relatively moderate time delay taken with respect to the extinction of the primary pulse.

The position and width of the time window during which the target signal may be seen, as well the position of the maximal target-to-overburden response ratio, depend primarily on the conductance contrast between the target and the overburden. They also depend upon the usual parameters such as target location and geometry and, to a lesser extent, on the geometry of the system. We have found that a closely coupled EM system can be expected to produce somewhat better results than a large-scale apparatus.

For a typical 300 by 300 m vertical conductor, the observation window is well defined once the conductance contrast between the conductor and the overburden exceeds 10. In that case, the time at which the window opens (τ_{early}) is only a function of the geometry and depth of the conductor. In a typical case where the overburden has a conductance of 1 S, a conductive target may be detected as early as 250 μs after the extinction of the primary field. Another point of interest is the time (τ_0) at which the target-to-overburden response ratio is a maximum. This quantity appears to be directly proportional to the conductance contrast between the target and the overburden. While this ratio (TOR) is also a function of target size, it seems to be largely independent of all other parameters. We note that, for magnetic field detection, the maximum TOR for a given conductor varies approximately as the cube of the conductance contrast. If voltage measurements are made, TOR_{max} depends more severely on the conductance contrast, rising as the fourth power of the conductance contrast.

For large conductance contrasts the temporal window during which the target may be observed is very wide, spanning nearly three decades of time. Because of practical considerations such as the available power, the natural electromagnetic noise, and the system noise, it is unlikely that one can plan to make measurements out to τ_{late}. Using the conventional stacking techniques (Macnae et al., 1984), one should, however, be able to detect the target signal between τ_{early} and τ_0 quite easily.

All of the above observations are consistent with a simple description for a target signal which decays exponentially at times greater than τ_{early}. This rudimentary model could be used to provide good estimates for the parameters of the observation window. The principal use of the model in this paper, however, is in the evaluation of corrections that must be made to TOR values required for a practical system that does not measure the step response. On the basis of the results shown, this model appears to be quite satisfactory for this purpose.

Comparing our results with those of Eaton and Hohmann (1987), we find good agreement on a number of key points. First, we see that the TOR for the magnetic field response at early times is greater than for the voltage response (in Eaton and Hohmann, 1987, these are referred to as the step and impulse responses, respectively). This large relative TOR holds true even for different transmitter-receiver configurations. Second, the time of maximum TOR for the magnetic field response is smaller than that for the voltage response. Our results, however, do not show that the magnetic field TOR should be greater than the voltage TOR, particularly at TOR_{max}. This disagreement relates to our use of an infinite overburden sheet model that shows a power-law decay of the secondary field, while Eaton and Hohmann (1987) use a finite overburden block model with an exponential decay.

Although the particular system configuration considered here is not yet widely used, the results should prove informative in other situations. The data required for evaluation of the performance of a given EM system in a given situation can be obtained numerically with an algorithm similar to that em-

Table 4. Comparison of predicted and theoretical or experimental TORs for the scale-model example in Figure 1; τ_1 is normalized time of measurement, VMF is voltage measurement modification to the TOR, PLF is finite current pulse length modification, MTF is the correction for a measurement at a time other than that of maximum TOR, TOR_{max} is the maximum target-to-overburden response ratio for the theoretical model, TOR_{pred} is the predicted TOR after the above corrections to TOR_{max}, TOR_{scale} is the TOR measured for the scale-model example (Figure 1), TOR_{SHEET} is the TOR determined from the SHEET program when using the scale-model parameters (except the overburden areal extent).

Comparison of TORs			
Channel	4	5	6
τ_1	4.62	6.51	8.79
VMF	0.26	0.36	0.49
PLF	0.77	0.80	0.86
MTF	0.33	0.52	0.75
TOR_{max}	1.8	1.8	1.8
TOR_{pred}	0.12	0.28	0.57
TOR_{scale}	0.15	0.34	0.60
TOR_{SHEET}	0.16	0.36	0.64

ployed to construct the SHEET program. Using these techniques, an explorationist can enhance his prospects of finding a buried conductor by optimizing the survey parameters to ensure signal detection in an appropriate time window.

ACKNOWLEDGMENTS

We would like to acknowledge the financial support of the Selco Division, BP Resources Canada Ltd., for this study. We would also like to thank Dr. Ki Ha Lee of Lawrence Berkeley Laboratory for his assistance in setting up the SHEET program.

REFERENCES

Bartel, D. C., and Hohmann, G. W., 1985, Interpretation of Crone pulse electromagnetic data: Geophysics, **50**, 1488–1499.

Becker, A., DeCarle, R., and Lazenby, P. G., 1984, Simplified prediction of transient electromagnetic response: Geophysics, **49**, 913–917.

Bosschart, R. A., and Seigel, H. O., 1965, Some aspects of the Turam electromagnetic method: Trans. Can. Inst. Mining Metall., **64**, 156–161.

Buselli, G., 1980, Interpretation of SIROTEM data from Elura, *in* Emerson, D. W., Ed., The geophysics of the Elura orebody, Cobar, New South Wales: Austral. Soc. Explor. Geophys., 122–129.

Dyck, A. V., Bloore, M., and Vallee, M. A., 1980, User manual for programs PLATE and SPHERE: Res. in Appl. Geophys. 14, Univ. of Toronto.

Eaton, P. A., and Hohmann, G. W., 1987, An evaluation of electromagnetic methods in the presence of geologic noise: Geophysics, **52**, 1106–1126.

Grant, F. S., and West, G. F., 1965, Interpretation theory in applied geophysics: McGraw-Hill Book Co., Inc.

Gupta Sarma, D., and Maru, V. M., 1971, A study of some effects of a conducting host rock with a new modelling apparatus: Geophys. Prosp., **36**, 166–183.

Gupta Sarma, D., Maru, V. M., and Varadarajan, G., 1976, An improved pulse transient airborne electromagnetic system for locating good conductors: Geophysics, **41**, 287–299.

Kaufman, A. A., 1981, The influence of currents induced in the host rock on electromagnetic response of a spheroid directly beneath a loop: Geophysics, **46**, 1121–1136.

Lamontagne, Y., 1975, Applications of wideband, time-domain EM measurements in mineral exploration: Res. in Appl. Geophys. 7, Univ. of Toronto.

Lazenby, P. G., 1973, New developments in the INPUT airborne E.M. system: Can. Inst. Mining Metall. Bull., **66**, no. 732, 96–104.

Macnae, J. C., Lamontagne, Y., and West, G. F., 1984, Noise processing techniques for time-domain electromagnetic systems: Geophysics, **49**, 934–948.

Mallick, K., 1972a, INPUT response to single-turn conductive circuit: Geoexplor., **10**, 255–259.

——— 1972b, Conducting sphere in electromagnetic input field: Geophys. Prosp., **20**, 293–303.

——— 1978, A note on the decay pattern of magnetic field and voltage response of conducting bodies in EM time-domain system: Geoexplor., **16**, 303–307.

McCracken, K. G., Oristaglio, M. L., and Hohmann, G. W., 1986, A comparison of electromagnetic exploration systems: Geophysics, **51**, 810–818.

Rai, S. S., 1985, Transient electromagnetic responses of a thin conducting plate embedded in conducting host rock: Geophysics, **50**, 1342–1349.

Spies, B. R., 1976, The derivation of absolute units in electromagnetic scale modeling: Geophysics, **41**, 1042–1049.

——— 1980a, TEM in Australian conditions: Field examples and model studies: Ph.D. thesis, Macquarie Univ.

——— 1980b, Interpretation and design of time-domain EM surveys in areas of conductive overburden, *in* Emerson, D. W., Ed., The geophysics of the Elura orebody, Cobar, New South Wales: Austral. Soc. Explor. Geophys., 130–139.

Weidelt, P., 1981, Report on dipole induction by a thin plate in a conductive halfspace with an overburden: Research proj. NTS 83 (BMFT), Fed. Int. for Earth Sciences and Raw Materials, Hannover, West Germany, archive no. 89727.

West, G. F., Macnae, J. C., and Lamontagne, Y., 1984, A time-domain EM system measuring the step response of the ground: Geophysics, **49**, 1010–1026.